Title

PEG-Infiltrated Polyoxometalate Frameworks with Flexible Form-Factors

Journal

ACS Materials Letters, 4(10)

ISSN

2639-4979

Authors

Alves, Liana S

Chen, Linfeng

Lemmon, Carl E

et al.

Publication Date

2022-10-03

DOI

10.1021/acsmaterialslett.2c00393

Peer reviewed

ACS MATERIALS LETTERS

www.acsmaterialsletters.org

PEG-Infiltrated Polyoxometalate Frameworks with Flexible Form-Factors

Liana S. Alves, Linfeng Chen, Carl E. Lemmon, Milan Gembicky, Mingjie Xu, and Alina M. Schimpf*

Cite This: *ACS Materials Lett.* 2022, 4, 1937−1943

Read Online

ACCESS | Metrics & More | Article Recommendations | Supporting Information

ABSTRACT: We present the synthesis of metal oxide frameworks composed of the Preyssler anion, $[NaP_5W_{30}O_{110}]^{14-}$, bridged with transition-metal cations and infiltrated with polyethylene glycol. The frameworks can be dissolved in water to form freestanding rigid or flexible films or gels. Powder X-ray diffraction shows that all form-factors maintain the short-range order of the original crystals. Raman spectroscopy reveals that, similar to hydrogels, the macroscopic mechanical properties of these composites are dependent on the water content and the extent of hydrogen-bonding within the water network. The understanding gained from these studies facilitates solution-phase processing of polyoxometalate frameworks into flexible form factors.

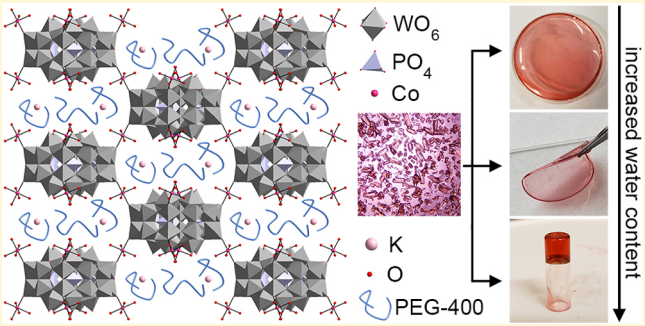

The construction of extended networks from molecular clusters has recently gained attention as a strategy for synthesizing new materials with precisely tailored atomic positions and rationally designed properties.[1−12] Polyoxometalates (POMs) are well-suited as anionic ligands for coordination networks because of their oxygen-rich surface, providing multiple coordination sites. Furthermore, POMs have immense structural and compositional variability, giving rise to unique electronic, magnetic, or photophysical properties,[13−17] as well as to rich, reversible redox activity.[13,14,17−19] Indeed, the assembly of POMs into coordination networks or other suprastructures has been increasingly used to access complex metal-oxide materials with diverse structures and functionalities.[3,5−7,20−38]

The synthesis of POMs and POM-based networks is usually performed to yield high-quality crystals or polycrystalline powders, but such form factors are not inherently suitable for many applications and may not be easily solution-processed. Advances in metal−organic framework research have enabled them to be processed into flexible form-factors through combination with polymers, often in mixed-matrix membranes.[39−41] Recently, POM−polymer composites have been used to combine the exciting properties of POMs with the facile processability and ductile nature of organic polymers, yielding hybrid materials with new functionalities.[42−46] A common strategy for composite formation is post-synthetic physical blending, but such mixtures are not held together well and can phase-segregate. Alternatively, electrostatic interactions have been used to promote composite assemblies, but these methods may be difficult to scale and are limited to charged polymers. Furthermore, these strategies have not been utilized for ordered, extended POM networks. Covalent functionalization of POMs has been used to access hybrid materials and networks, but these methods can be synthetically challenging and are not viable for all POMs.

We report the synthesis of a polymer-infiltrated POM framework, crystals of which can be processed into various form-factors. Specifically, a framework composed of the Preyssler anion, $[NaP_5W_{30}O_{110}]^{14-}$ (denoted as $\{P_5W_{30}\}$),[47] bridged with transition-metal ions and infiltrated with polyethylene glycol (PEG) is presented (Figure 1). Crystals of these frameworks show remarkable stability toward desolvation, compared to those without PEG. Importantly, the crystals can be dissolved in water to form gels or to be recast as films, with all form-factors displaying short-range order analogous to that of the original crystals. Electron microscopy images reveal that, unlike physically blended composites, films presented herein are homogeneous on the submicrometer scale. The mechanical properties of the films are dependent on the humidity, allowing for reversible switching between rigid and flexible states. Using Raman

Received: May 4, 2022
Accepted: August 5, 2022
Published: September 6, 2022

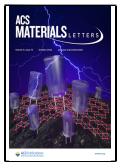

https://doi.org/10.1021/acsmaterialslett.2c00393
ACS Materials Lett. 2022, 4, 1937−1943

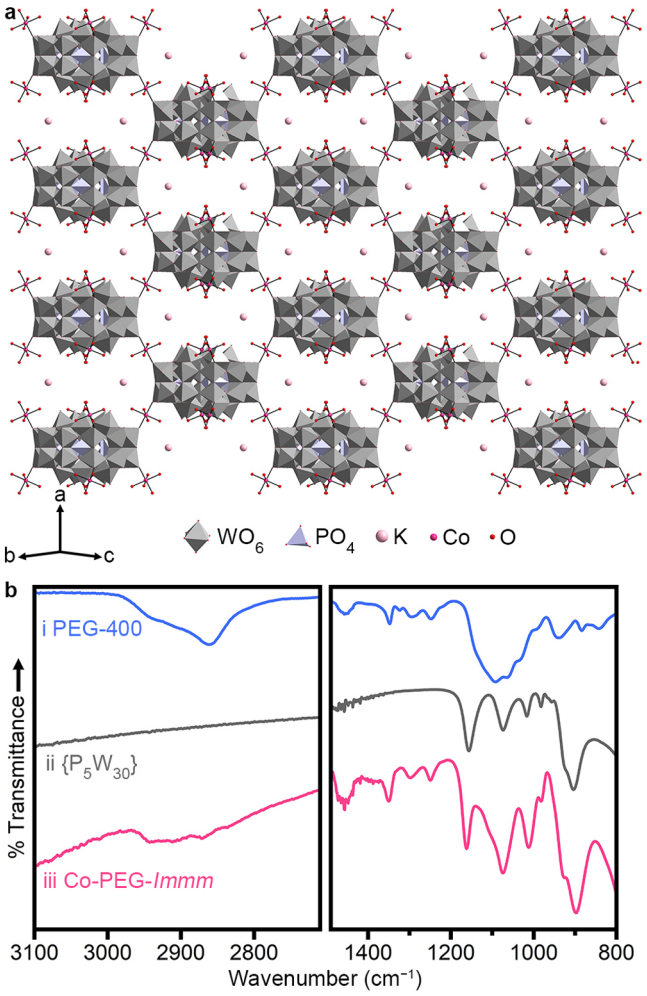

Figure 1. (a) Crystal structure of PEG-containing Co-bridged $\{P_5W_{30}\}$ (Co-PEG-*Immm*). (b) IR absorption spectra of (i) PEG-400, (ii) $\{P_5W_{30}\}$, and (iii) crushed, washed crystals of Co-PEG-*Immm*.

spectroscopy, we show that increased flexibility is due to higher water content, which corresponds to a decrease in hydrogen bonding within these framework−PEG−water composites. These experiments elucidate the factors important to achieving flexible form-factors with POM-based frameworks and ultimately facilitate their solution-phase processing for a wide range of applications.

PEG-containing frameworks (Figure 1) were synthesized using the same methods as used for non-PEG frameworks,[36−38] with the addition of PEG during the crystallization stage. Briefly, $K_{14-x}Na_x[NaP_5W_{30}O_{110}]$ and $CoCl_2{\cdot}6H_2O$ were added to 1 M aqueous LiCl and the solution was refluxed for ∼12 h. Upon cooling to room temperature, PEG-400 (120 equiv/$\{P_5W_{30}\}$) was added to the solution and crystals were grown via methanol (MeOH) diffusion into the solution. The resulting crystals have a structure that is distinct from those obtained without PEG.[36−38] Figure 1a shows the crystal structure of frameworks synthesized with $CoCl_2{\cdot}6H_2O$, which yielded pink crystals with an orthorhombic *Immm* unit cell (Co-PEG-*Immm*; Table S1; a = 17.9869(7) Å, b = 21.8213(8) Å, and c = 24.8909(10) Å). Each $\{P_5W_{30}\}$ is connected to eight, crystallographically equivalent neighboring clusters through the $Co(H_2O)_4^{2+}$ bridging ions (Figures 1a and S1). Electron density in the void space of the structure is assigned to K^+ (2 per $\{P_5W_{30}\}$), which is likely coordinated by a combination O from PEG and water.

Although PEG cannot be assigned crystallographically, IR spectroscopy reveals that the polymer is present even after the crystals are crushed and extensively washed (Figure 1b), suggesting that PEG incorporates into the void space of the framework. It is likely that the PEG wraps around the K^+ within the pores.[48] Importantly, inclusion of PEG imparts additional stability of the framework against desolvation. Unlike our previous $\{P_5W_{30}\}$-based frameworks, which contract upon removal from the mother liquor,[36] the structure of Co-PEG-*Immm* is largely unchanged upon removal from the mother liquor (Figure S2). Elemental analysis was used to estimate a formula of $H_{1.5}Li_{1.5}NaK_2Co_4[NaP_5W_{30}O_{110}]{\cdot}3PEG{\cdot}24.5H_2O$. This polymer content is higher than most $\{P_5W_{30}\}$-based composites,[49−52] but is consistent with the void space of the framework. Based on the crystal structure, the void space is calculated to be ∼2500 Å^3 per $\{P_5W_{30}\}$, which could fit up to ∼4 PEG-400 molecules (Table S2). Crystallization with larger polymers that do not fit in the void space of the framework did not readily yield polymer-infiltrated crystals.

We note that the structure presented in Figure 1a is simplified by showing only one of the two disordered cluster configurations. In addition, cations found in elemental analysis cannot be assigned crystallographically because of large disorder. This high level of disorder is typical of POM-based coordination networks and is seen in some previous $\{P_5W_{30}\}$ frameworks.[36−38]

Analogous synthetic conditions can be used to obtain isostructural *Immm* frameworks with $M(H_2O)_4^{n+}$ (M^{n+} = Mn^{2+}, $Fe^{2+/3+}$, Ni^{2+}, Zn^{2+}) bridging ions (Table S1, Figures S3 and S4). When the same synthesis was performed with $CuCl_2{\cdot}6H_2O$, however, isostructural frameworks were not initially obtained (Figure S3). Instead, the resulting crystals are composed of $Cu(H_2O)_5^{2+}$-decorated $\{P_5W_{30}\}$ with an orthorhombic $C222_1$ unit cell (Table S3 and Figure S5). IR spectroscopy of crushed and washed crystals revealed that all ($M(H_2O)_4^{n+}$-bridged and $Cu(H_2O)_5^{2+}$-decorated) contained PEG (Figure S5).

Importantly, the incorporation of PEG into these $\{P_5W_{30}\}$-based frameworks enables facile processing of the framework architecture into various form-factors. When crystals of Co-PEG-*Immm* (Figure 2a, trace i) were dissolved in water, the resulting solution could be drop-cast into films that are rigid (Figure 2a, trace ii) or flexible (Figure 2a, trace iii), depending on the humidity (<60% for rigid films, 60%−85% for flexible films). The films are free-standing and can be reversibly switched between the rigid and flexible forms using a humidity chamber or heat. Both the rigid and flexible forms maintain the short-range order found in the original crystals (Figure 2a). This ordering can also be seen in medium-angle annular dark field scanning transmission electron microscopy (MAADF-STEM) images of a rigid film (Figure S6). We note that PEG-400 is a liquid, and thus the films cannot simply be microcrystallites embedded in the PEG matrix. This claim is corroborated by scanning electron microscopy (SEM) imaging, which reveals that the films are homogeneous on the submicrometer scale (Figure S7).

Films could also be cast from other M-PEG-*Immm* frameworks (Figure 2b; M = Mn, Fe, Ni, Zn), which all show the same diffraction as that of films cast from Co-PEG-*Immm* (Figure S8). Interestingly, films cast from Cu-decorated

https://doi.org/10.1021/acsmaterialslett.2c00393
ACS Materials Lett. 2022, 4, 1937−1943

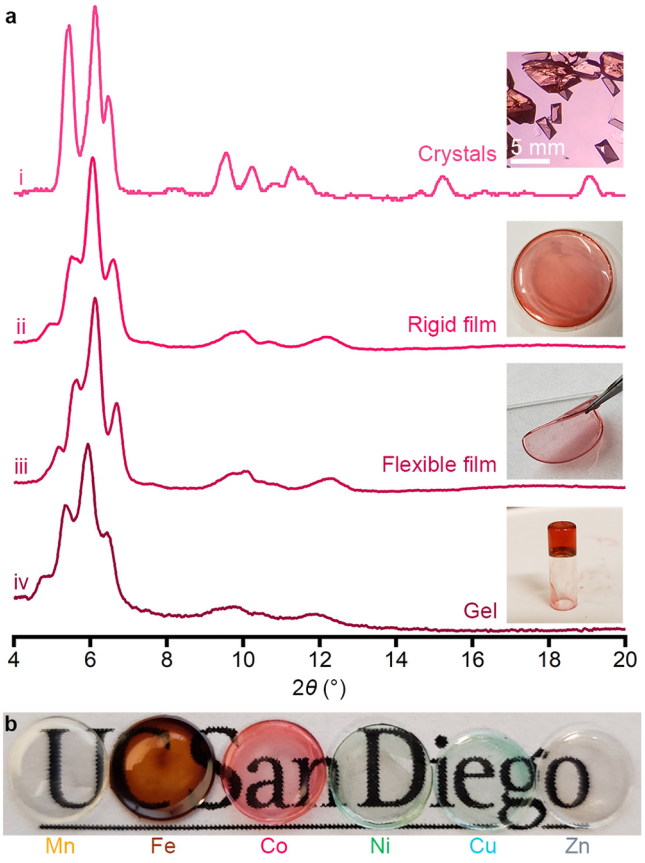

Figure 2. (a) Powder X-ray diffraction patterns and photographs of (i) Co-PEG-*Immm* crystals, Co-PEG-*Immm* cast into a film at (ii) ~50% humidity (rigid, film diameter of ~35 mm) and (iii) ~60% humidity (flexible, film diameter of ~15 mm), and (iv) Co-PEG-*Immm* dissolved in ~50 equiv water and heated to form a gel. Insets show photographs of each form factor. (b) Photograph of PEG-containing (left to right) Mn-, Fe-, Co-, Ni-, Cu-, and Zn-bridged $\{P_5W_{30}\}$ cast into films at ~50% humidity. Each film is ~8 mm in diameter.

clusters (Figure 2b) also show the same ordering as those cast from M-PEG-*Immm* frameworks (Figure S8).

The dependence of macroscopic mechanical properties on the humidity (i.e., water-content) is reminiscent of hydrogels, although our materials would dissolve if submerged in water. Indeed, the dissolution of concentrated Co-PEG-*Immm* forms a gel-like substance that does not flow but has short-range order similar to that of the crystals and films (Figure 2a, trace iv). The gel-like behavior of this form-factor was verified using parallel-plate rheological measurements. Figure 3 shows the storage (G', closed circles) and loss (G'', open circles) moduli as a function of angular frequency (ω) measured at 2.6% strain. The observation of relatively flat moduli with $G' > G''$ confirms the gel-like nature under these measurement conditions, although with a relatively low ratio of G'/G''.[53−59] These gels are unique from previously reported "gel-like" POM−polymer coacervates, which did not diffract and behaved as viscoelastic liquids.[60] Solid- and rubber-like composites have been formed with polyoxovanadates and gelatin, but do not contain an ordered, extended structure.[61]

To evaluate the importance of the various components in accessing the varied form-factors, several controls were performed. First, PEG-free frameworks (Co-*Imma*)[36,37] could not be cast into films using the same method, but instead

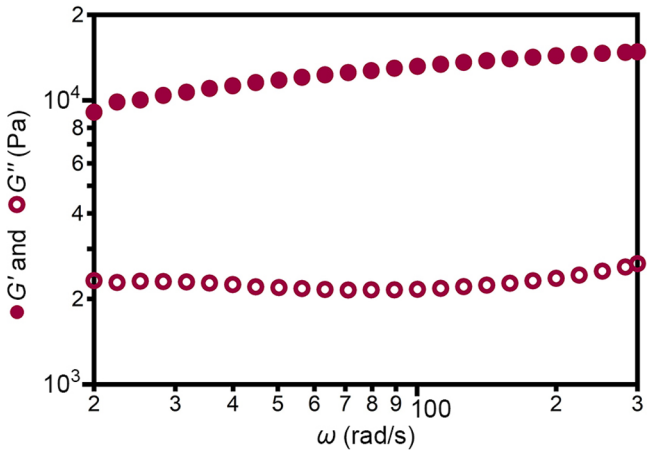

Figure 3. Storage (G', closed circles) and loss (G'', open circles) moduli of the gel form-factor as a function of angular frequency (ω).

resulted in a polycrystalline powder (Figure S9a). Similarly, we were unable to form homogeneous films from Co-*Imma* frameworks dissolved in water and mixed with PEG (Figure S9b), or from an aqueous mixture of $CoCl_2$, $\{P_5W_{30}\}$, and PEG (Figure S9c). Finally, we synthesized PEG-infiltrated $\{P_5W_{30}\}$ crystals (PEG-$\{P_5W_{30}\}$, Table S3 and Figure S10). When these crystals were dissolved in water, they could be cast into free-standing rigid films (Figure S10) with ordering different than the parent crystals. However, these films are not transparent and cannot be made flexible. Instead, increased humidity causes the films to break apart and eventually dissolve. These controls highlight the importance of the Co-bridged framework structure as well as the PEG in enabling access to various form-factors that maintain structural integrity. Indeed, the coordination mode of countercations was recently shown to play a crucial role in the formation of POM-based organogels.[62]

An important factor in the formation and mechanical properties of polymer-based hydrogels is the hydrogen-bonding network of the water molecules, which can be monitored using Raman spectroscopy.[63−67] Figure 4 shows the Raman spectra of the various form-factors of Co-PEG-*Immm*.

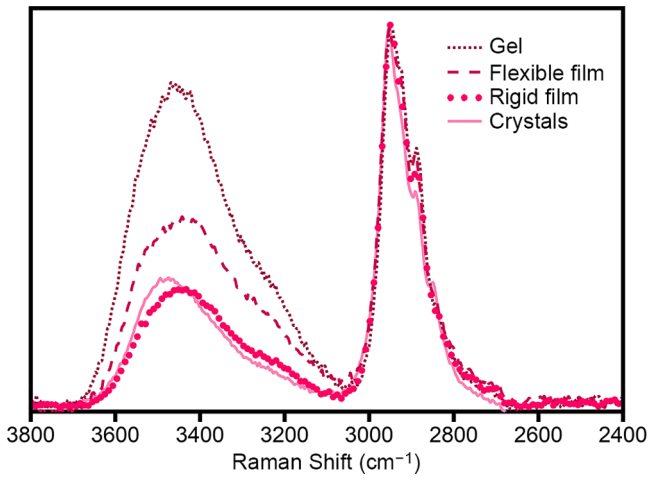

Figure 4. Raman spectra of Co-PEG-*Immm* crystals and of the flexible film, rigid film, and gel forms. Spectra are normalized to the C−H modes of PEG (~2900 cm^{-1}).

https://doi.org/10.1021/acsmaterialslett.2c00393
ACS Materials Lett. 2022, 4, 1937−1943

In these spectra, the peaks at ~2700−3000 cm^{-1} are assigned to the C−H modes of PEG[68] and the intensity at ~3100−3700 cm^{-1} is due to several overlapping water modes (Table S4, vide infra).[65−67,69−72] Since each form-factor contains the same amount of PEG, the spectra are normalized to the C−H modes of PEG. Based on the envelope of water modes, the relative water content increases as crystals ≈ rigid film < flexible film < gel.

The envelope of water modes in the Raman spectra can be further analyzed to determine the relative amount of hydrogen bonding. The Raman spectrum of pure H_2O is shown in Figure 5, trace i. This spectrum contains several water modes for

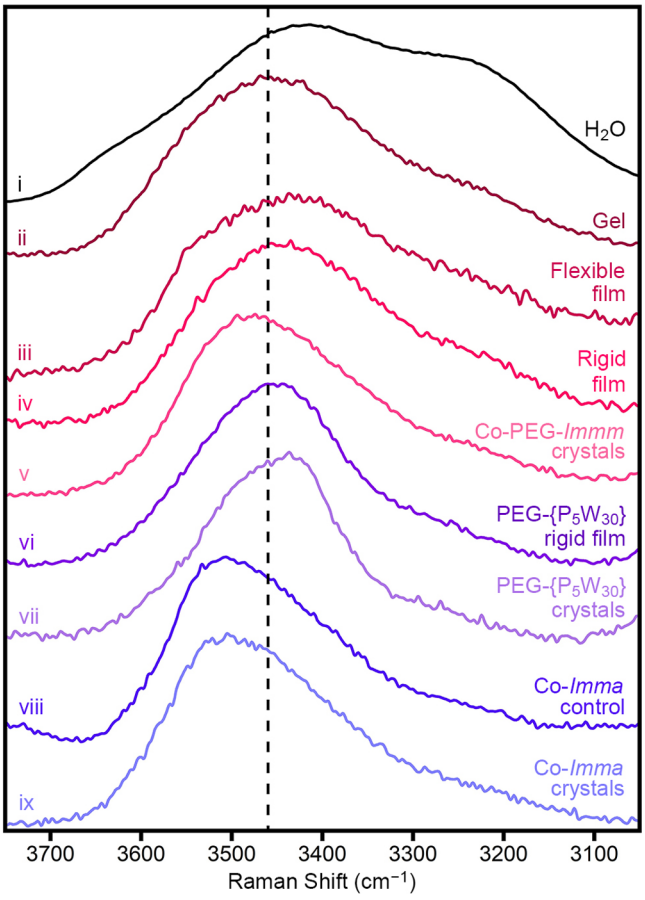

Figure 5. Raman spectra of (i) water, (ii) gel, (iii) flexible film, and (iv) rigid film forms derived from (v) Co-PEG-*Immm* crystals. (vi) rigid film cast from (vii) PEG-{P_5W_{30}} crystals. Control attempts to cast a (viii) film from (ix) Co-*Imma* crystals. The dashed vertical line indicates the isosbestic point for strongly versus weakly/non-hydrogen-bound water.

strongly hydrogen-bound and weakly/non-hydrogen-bound water (Table S4).[65−67,69−72] The dashed line at 3460 cm^{-1} is the isosbestic point, at which the Raman scattering is insensitive to the change in the amount/strength of hydrogen bonding.[69] In other words, this line demarcates the strongly and weakly/non-hydrogen-bonding regimes. An increase in intensity to the right of this line (lower wavenumber) is indicative of greater hydrogen bonding, while increased intensity to the left (higher wavenumber) is indicative of lesser hydrogen bonding. To compare the amount/strength of hydrogen bonding between samples, the ratios of integrated intensities of the strongly hydrogen-bound region (3100−3460 cm^{-1}) and weakly/non-hydrogen-bound (3460−3750 cm^{-1}) were used (Table S5). From these data, it can be seen that the gel (Figure 5, trace ii), flexible film (Figure 5, trace iii), and rigid film (Figure 5, trace iv) have increased hydrogen bonding, compared to the parent crystals (Figure 5, trace v). Furthermore, the hydrogen bonding increases as gel < flexible film < rigid film. This trend is consistent with that observed in the swelling of polymer-based hydrogels, where increased water is added as "free" water, leading to an overall decrease in the ratio of hydrogen-bound/non-hydrogen-bound water.[65−67] Thus, the hydrogel-like forms of Co-PEG-*Immm* show an increase in hydrogen bonding, relative to their parent crystals. In contrast, this increase in hydrogen bonding is not seen in the rigid PEG-{P_5W_{30}} film (Figure 5, trace vi) compared to the parent PEG-{P_5W_{30}} crystals (Figure 5, trace vii). Although the Co-PEG-*Immm* and PEG-{P_5W_{30}} crystals have similar levels of hydrogen bonding, film formation from PEG-{P_5W_{30}} does not lead to an increase in hydrogen bonding, preventing access to flexible form-factors. Similarly, no increase in hydrogen bonding is seen when we attempt to cast films (Co-*Imma* control, Figure 5, trace viii; Figure S9) from Co-*Imma* crystals (Figure 5, trace ix), which do not contain PEG. We note that both Co-PEG-*Immm* and PEG-{P_5W_{30}} crystals contain more hydrogen bonding than Co-*Imma* crystals, highlighting the importance of PEG in enabling the formation of the hydrogen-bound water-network. Overall, these data suggest that the many components of the Co^{2+}-bridged frameworks are important for accessing the increased hydrogen bonding that enables flexible and switchable form-factors.

In summary, we have demonstrated that transition-metal bridged {P_5W_{30}} frameworks can be infiltrated with PEG to (i) imbue increased stability toward desolvation and (ii) enable facile, solution-phase processing into form-factors with various macroscopic mechanical properties. Similar to hydrogels, the flexibility of these materials is dependent on the amount of water trapped in the composites and on the extent of hydrogen bonding within the water network. These experiments elucidate factors that enable solution-phase processing of polyoxometalate-based frameworks into various form-factors.

■ ASSOCIATED CONTENT

Supporting Information

The Supporting Information is available free of charge at https://pubs.acs.org/doi/10.1021/acsmaterialslett.2c00393.

Supplementary tables and figures; experimental details including synthesis and characterization (PDF)

Structural data for the PEG-infiltrated, Co-bridged framework $H_zLi_yNa_xK_{6-x-y-z}Co_4[NaP_5W_{30}O_{110}]\cdot mPEG\cdot n H_2O$ (Co-PEG-*Immm*) (CIF)

Structural data for the PEG-infiltrated, Mn-bridged framework $H_zLi_yNa_xK_{5-x-y-z}Mn_{4.5}[NaP_5W_{30}O_{110}]\cdot mPEG\cdot n H_2O$ (Mn-PEG-*Immm*) (CIF)

Structural data for the PEG-infiltrated, Fe-bridged framework $H_zLi_yNa_xK_{5-x-y-z}Fe_{4.5}[NaP_5W_{30}O_{110}]\cdot mPEG\cdot n H_2O$ (Fe-PEG-*Immm*) (CIF)

Structural data for the PEG-infiltrated, Ni-bridged framework $H_zLi_yNa_xK_{5-x-y-z}Ni_{4.5}[NaP_5W_{30}O_{110}]\cdot mPEG\cdot n H_2O$ (Ni-PEG-*Immm*) (CIF)

Structural data for the PEG-infiltrated, Zn-bridged framework $H_zLi_yNa_xK_{6-x-y-z}Zn_4[NaP_5W_{30}O_{110}]\cdot mPEG\cdot n H_2O$ (Zn-PEG-*Immm*) (CIF)

https://doi.org/10.1021/acsmaterialslett.2c00393
ACS Materials Lett. 2022, 4, 1937−1943

Structural data for the PEG-infiltrated, Cu-decorated Preyssler $H_zLi_yNa_xK_{6-x-y-z}Cu_4[NaP_5W_{30}O_{110}]\cdot mPEG\cdot n H_2O$ (Cu-PEG-C222$_1$) (CIF)

Structural data for the PEG-infiltrated Preyssler $H_zLi_yNa_xK_{14-x-y-z}[NaP_5W_{30}O_{110}]\cdot mPEG\cdot n H_2O$ (PEG-{P_5W_{30}}) (CIF)

Accession Codes

Cambridge Structural Database codes for all deposited CIFs are reported in Tables S1 and S3. These data can be obtained free of charge via www.ccdc.cam.ac.uk/data_request/cif, or by emailing data_request@ccdc.cam.ac.uk, or by contacting The Cambridge Crystallographic Data Centre, 12 Union Road, Cambridge CB21EZ, UK; fax: + 44 1223 336033.

AUTHOR INFORMATION

Corresponding Author

Alina M. Schimpf − *Department of Chemistry and Biochemistry, University of California, San Diego, La Jolla, California 92093, United States;* orcid.org/0000-0001-5402-7426; Email: aschimpf@ucsd.edu

Authors

Liana S. Alves − *Department of Chemistry and Biochemistry, University of California, San Diego, La Jolla, California 92093, United States*

Linfeng Chen − *Department of Chemistry and Biochemistry, University of California, San Diego, La Jolla, California 92093, United States;* orcid.org/0000-0002-0436-3197

Carl E. Lemmon − *Department of Chemistry and Biochemistry, University of California, San Diego, La Jolla, California 92093, United States*

Milan Gembicky − *Department of Chemistry and Biochemistry, University of California, San Diego, La Jolla, California 92093, United States*

Mingjie Xu − *Irvine Materials Research Institute, University of California, Irvine, California 92697, United States*

Complete contact information is available at: https://pubs.acs.org/10.1021/acsmaterialslett.2c00393

Notes

The authors declare no competing financial interest.

ACKNOWLEDGMENTS

This research was supported by the U.S. National Science Foundation (DMR-2046269 to A.M.S.). Rheology measurements were performed using facilities supported by the NSF through the UC San Diego Materials Research Science and Engineering Center (UCSD MRSEC, DMR-2011924). SEM measurements were performed using facilities supported by the San Diego Nanotechnology Infrastructure (SDNI), a member of the National Nanotechnology Coordinated Infrastructure (ECCS-1542148). STEM data were collected at the UC Irvine Materials Research Institute (IMRI), which is supported in part by the NSF through the UC Irvine Materials Research Science and Engineering Center (DMR-2011967).

REFERENCES

(1) Yaghi, O. M.; Sun, Z.; Richardson, D. A.; Groy, T. L. Directed Transformation of Molecules to Solids - Synthesis of a Microporous Sulfide from Molecular Germanium Sulfide Cages. *J. Am. Chem. Soc.* **1994**, *116*, 807.

(2) Zheng, Z. P.; Long, J. R.; Holm, R. H. A Basis Set of Re_6Se_8 Cluster Building Blocks and Demonstration of Their Linking Capability: Directed Synthesis of an $Re_{12}Se_{16}$ Dicluster. *J. Am. Chem. Soc.* **1997**, *119*, 2163.

(3) Long, D. L.; Burkholder, E.; Cronin, L. Polyoxometalate Clusters, Nanostructures and Materials: From Self Assembly to Designer Materials and Devices. *Chem. Soc. Rev.* **2007**, *36*, 105.

(4) Cairns, A. J.; Perman, J. A.; Wojtas, L.; Kravtsov, V. C.; Alkordi, M. H.; Eddaoudi, M.; Zaworotko, M. J. Supermolecular Building Blocks (SBBs) and Crystal Design: 12-Connected Open Frameworks Based on a Molecular Cubohemioctahedron. *J. Am. Chem. Soc.* **2008**, *130*, 1560.

(5) Miras, H. N.; Vila-Nadal, L.; Cronin, L. Polyoxometalate Based Open-Frameworks (POM-OFs). *Chem. Soc. Rev.* **2014**, *43*, 5679.

(6) Boyd, T.; Mitchell, S. G.; Gabb, D.; Long, D. L.; Song, Y. F.; Cronin, L. POMzites: A Family of Zeolitic Polyoxometalate Frameworks from a Minimal Building Block Library. *J. Am. Chem. Soc.* **2017**, *139*, 5930.

(7) Vilà-Nadal, L.; Cronin, L. Design and Synthesis of Polyoxometalate-Framework Materials from Cluster Precursors. *Nat. Rev. Mater.* **2017**, *2*, 17054.

(8) Horwitz, N. E.; Xie, J. Z.; Filatov, A. S.; Papoular, R. J.; Shepard, W. E.; Zee, D. Z.; Grahn, M. P.; Gilder, C.; Anderson, J. S. Redox-Active 1D Coordination Polymers of Iron-Sulfur Clusters. *J. Am. Chem. Soc.* **2019**, *141*, 3940.

(9) Kephart, J. A.; Romero, C. G.; Tseng, C. C.; Anderton, K. J.; Yankowitz, M.; Kaminsky, W.; Velian, A. Hierarchical Nanosheets Built From Superatomic Clusters: Properties, Exfoliation and Single-Crystal-to-Single-Crystal Intercalation. *Chem. Sci.* **2020**, *11*, 10744.

(10) Gadjieva, N. A.; Champsaur, A. M.; Steigerwald, M. L.; Roy, X.; Nuckolls, C. Dimensional Control of Assembling Metal Chalcogenide Clusters. *Eur. J. Inorg. Chem.* **2020**, *2020*, 1245.

(11) Bartholomew, A. K.; Meirzadeh, E.; Stone, I. B.; Koay, C. S.; Nuckolls, C.; Steigerwald, M. L.; Crowther, A. C.; Roy, X. Superatom Regiochemistry Dictates the Assembly and Surface Reactivity of a Two-Dimensional Material. *J. Am. Chem. Soc.* **2022**, *144*, 1119.

(12) Gillen, J. H.; Moore, C. A.; Vuong, M.; Shajahan, J.; Anstey, M. R.; Alston, J. R.; Bejger, C. M. Synthesis and Disassembly of an Organometallic Polymer Comprising Redox-Active Co_4S_4 Clusters and Janus Biscarbene Linkers. *Chem. Commun.* **2022**, *58*, 4885.

(13) Pope, M. T.; Muller, A. Polyoxometalate Chemistry: An Old Field with New Dimensions in Several Disciplines. *Angew. Chem., Int. Ed.* **1991**, *30*, 34.

(14) Yamase, T. Photo- and Electrochromism of Polyoxometalates and Related Materials. *Chem. Rev.* **1998**, *98*, 307.

(15) Lopez, X.; Carbo, J. J.; Bo, C.; Poblet, J. M. Structure, Properties and Reactivity of Polyoxometalates: A Theoretical Perspective. *Chem. Soc. Rev.* **2012**, *41*, 7537.

(16) Cronin, L.; Muller, A. From Serendipity to Design of Polyoxometalates at the Nanoscale, Aesthetic Beauty and Applications. *Chem. Soc. Rev.* **2012**, *41*, 7333.

(17) Gumerova, N. I.; Rompel, A. Synthesis, Structures and Applications of Electron-Rich Polyoxometalates. *Nat. Rev. Chem.* **2018**, *2*, 0112.

(18) VanGelder, L. E.; Brennessel, W. W.; Matson, E. M. Tuning the Redox Profiles of Polyoxovanadate-Alkoxide Clusters via Heterometal Installation: Toward Designer Redox Reagents. *Dalton Trans* **2018**, *47*, 3698.

(19) Chen, J. J.; Symes, M. D.; Cronin, L. Highly Reduced and Protonated Aqueous Solutions of $[P_2W_{18}O_{62}]^{6-}$ for On-Demand Hydrogen Generation and Energy Storage. *Nat. Chem.* **2018**, *10*, 1042.

(20) Khan, M. I.; Yohannes, E.; Doedens, R. J. $[M_3V_{18}O_{42}(H_2O)_{12}(XO_4)]\cdot 24H_2O$ (M = Fe, Co; X = V, S): Metal Oxide Based Framework Materials Composed of Polyoxovanadate Clusters. *Angew. Chem., Int. Ed.* **1999**, *38*, 1292.

(21) Lu, Y.; Li, Y. G.; Wang, E. B.; Xu, X. X.; Ma, Y. A New Family of Polyoxometalate Compounds Built up of Preyssler Anions and Trivalent Lanthanide Cations. *Inorg. Chim. Acta* **2007**, *360*, 2063.

(22) Ritchie, C. I.; Streb, C.; Thiel, J.; Mitchell, S. G.; Miras, H. N.; Long, D. L.; Boyd, T.; Peacock, R. D.; McGlone, T.; Cronin, L.

Reversible Redox Reactions in an Extended Polyoxometalate Framework Solid. *Angew. Chem., Int. Ed.* **2008**, *47*, 6881.
(23) Mitchell, S. G.; Gabb, D.; Ritchie, C.; Hazel, N.; Long, D. L.; Cronin, L. Controlling Nucleation of the Cyclic Heteropolyanion $\{P_8W_{48}\}$: A Cobalt-Substituted Phosphotungstate Chain and Network. *Crys. Eng. Comm.* **2009**, *11*, 36.
(24) Zhang, Z. M.; Yao, S.; Li, Y. G.; Shi, Q.; Wang, E. B. A 1-D Ladder-Like Aggregate Constructed from Preyssler Anion and Transition Metal Linkers. *J. Coord. Chem.* **2009**, *62*, 3259.
(25) Bassil, B. S.; Ibrahim, M.; Mal, S. S.; Suchopar, A.; Biboum, R. N.; Keita, B.; Nadjo, L.; Nellutla, S.; van Tol, J.; Dalal, N. S.; Kortz, U. Cobalt, Manganese, Nickel, and Vanadium Derivatives of the Cyclic 48-Tungsto-8-Phosphate $[H_7P_8W_{48}O_{184}]^{33-}$. *Inorg. Chem.* **2010**, *49*, 4949.
(26) Long, D. L.; Tsunashima, R.; Cronin, L. Polyoxometalates: Building Blocks for Functional Nanoscale Systems. *Angew. Chem., Int. Ed.* **2010**, *49*, 1736.
(27) Mitchell, S. G.; Streb, C.; Miras, H. N.; Boyd, T.; Long, D. L.; Cronin, L. Face-Directed Self-Assembly of an Electronically Active Archimedean Polyoxometalate Architecture. *Nat. Chem.* **2010**, *2*, 308.
(28) Zhang, L. C.; Xue, H.; Zhu, Z. M.; Zhang, Z. M.; Li, Y. G.; Wang, E. B. Two New $\{P_8W_{49}\}$ Wheel-Shaped Tungstophosphates Decorated by Co(II), Ni(II) Ions. *J. Clust. Sci.* **2010**, *21*, 679.
(29) Chen, S. W.; Boubekeur, K.; Gouzerh, P.; Proust, A. Versatile Host−Guest Chemistry and Networking Ability of the Cyclic Tungstophosphate $\{P_8W_{48}\}$: Two Further Manganese Derivatives. *J. Mol. Struct.* **2011**, *994*, 104.
(30) Hutin, M.; Long, D. L.; Cronin, L. Controlling the Molecular Assembly of Polyoxometalates from the Nano to the Micron Scale: Molecules to Materials. *Isr. J. Chem.* **2011**, *51*, 205.
(31) Mitchell, S. G.; Boyd, T.; Miras, H. N.; Long, D. L.; Cronin, L. Extended Polyoxometalate Framework Solids: Two Mn(II)-Linked $\{P_8W_{48}\}$ Network Arrays. *Inorg. Chem.* **2011**, *50*, 136.
(32) von Allmen, K. D.; Grundmann, H.; Linden, A.; Patzke, G. R. Synthesis and Characterization of 0D−3D Copper-Containing Tungstobismuthates Obtained from the Lacunary Precursor $Na_9[B\text{-}\alpha\text{-}BiW_9O_{33}]$. *Inorg. Chem.* **2017**, *56*, 327.
(33) Zhan, C. H.; Cameron, J. M.; Gabb, D.; Boyd, T.; Winter, R. S.; Vila-Nadal, L.; Mitchell, S. G.; Glatzel, S.; Breternitz, J.; Gregory, D. H.; Long, D. L.; Macdonell, A.; Cronin, L. A Metamorphic Inorganic Framework that can be Switched Between Eight Single-Crystalline States. *Nat. Commun.* **2017**, *8*, 14185.
(34) Cronin, L.; Zhan, C.-H.; Zheng, Q.; Long, D. L.; Vila-Nadal, L. Controlling the Reactivity of the $[P_8W_{48}O_{184}]^{40-}$ Inorganic Ring and Its Assembly into POMZite Inorganic Frameworks with Silver Ions. *Angew. Chem., Int. Ed.* **2019**, *131*, 17442.
(35) Liu, Q. D.; He, P. L.; Yu, H. D.; Gu, L.; Ni, B.; Wang, D.; Wang, X. Single Molecule-Mediated Assembly of Polyoxometalate Single-Cluster Rings and Their Three-Dimensional Superstructures. *Sci. Adv.* **2019**, *5*, 1081.
(36) Turo, M. J.; Chen, L.; Moore, C. E.; Schimpf, A. M. Co^{2+}-Linked $[NaP_5W_{30}O_{110}]^{14-}$: A Redox-Active Metal Oxide Framework with High Electron Density. *J. Am. Chem. Soc.* **2019**, *141*, 4553.
(37) Chen, L.; San, K. A.; Turo, M. J.; Gembicky, M.; Fereidouni, S.; Kalaj, M.; Schimpf, A. M. Tunable Metal Oxide Frameworks via Coordination Assembly of Preyssler-Type Molecular Clusters. *J. Am. Chem. Soc.* **2019**, *141*, 20261.
(38) Chen, L.; Turo, M. J.; Gembicky, M.; Reinicke, R. A.; Schimpf, A. M. Cation-Controlled Assembly of Polyoxotungstate-Based Coordination Networks. *Angew. Chem., Int. Ed.* **2020**, *59*, 16609.
(39) Denny, M. S.; Moreton, J. C.; Benz, L.; Cohen, S. M. Metal−Organic Frameworks for Membrane-Based Separations. *Nat. Rev. Mater.* **2016**, *1*, 16078.
(40) Kalaj, M.; Cohen, S. M. Postsynthetic Modification: An Enabling Technology for the Advancement of Metal−Organic Frameworks. *ACS Cent. Sci.* **2020**, *6*, 1046.
(41) Jia, S. Y.; Ji, D. X.; Wang, L. M.; Qin, X. H.; Ramakrishna, S. Metal−Organic Framework Membranes: Advances, Fabrication, and Applications. *Small Struct* **2022**, *3*, 2100222.
(42) Qi, W.; Wu, L. X. Polyoxometalate/Polymer Hybrid Materials: Fabrication and Properties. *Polym. Int.* **2009**, *58*, 1217.
(43) Genovese, M.; Lian, K. Polyoxometalate Modified Inorganic-Organic Nanocomposite Materials for Energy Storage Applications: A Review. *Curr. Opin. Solid. St. M.* **2015**, *19*, 126.
(44) Li, B.; Li, W.; Li, H. L.; Wu, L. X. Ionic Complexes of Metal Oxide Clusters for Versatile Self Assemblies. *Acc. Chem. Res.* **2017**, *50*, 1391.
(45) Yan, J.; Zheng, X. W.; Yao, J. H.; Xu, P.; Miao, Z. L.; Li, J. L.; Lv, Z. D.; Zhang, Q. Y.; Yan, Y. Metallopolymers From Organically Modified Polyoxometalates (MOMPs): A Review. *J. Organomet. Chem.* **2019**, *884*, 1.
(46) Cameron, J. M.; Guillemot, G.; Galambos, T.; Amin, S. S.; Hampson, E.; Mall Haidaraly, K.; Newton, G. N.; Izzet, G. Supramolecular Assemblies of Organo-Functionalised Hybrid Polyoxometalates: From Functional Building Blocks to Hierarchical Nanomaterials. *Chem. Soc. Rev.* **2022**, *51*, 293.
(47) Alizadeh, M. H.; Harmalker, S. P.; Jeannin, Y.; Martinfrere, J.; Pope, M. T. A Heteropolyanion with Fivefold Molecular Symmetry That Contains a Nonlabile Encapsulated Sodium-Ion - the Structure and Chemistry of $[NaP_5W_{30}O_{110}]^{14-}$. *J. Am. Chem. Soc.* **1985**, *107*, 2662.
(48) Walsh, R. D.; Smith, J. M.; Hanks, T. W.; Pennington, W. T. Computational and Crystallographic Studies of Pseudo-Polyhalides. *Cryst. Growth Des.* **2012**, *12*, 2759.
(49) Niinomi, K.; Miyazawa, S.; Hibino, M.; Mizuno, N.; Uchida, S. High Proton Conduction in Crystalline Composites Based on Preyssler-Type Polyoxometalates and Polymers under Nonhumidified or Humidified Conditions. *Inorg. Chem.* **2017**, *56*, 15187.
(50) Iwano, T.; Miyazawa, S.; Osuga, R.; Kondo, J. N.; Honjo, K.; Kitao, T.; Uemura, T.; Uchida, S. Confinement of Poly(allylamine) in Preyssler-Type Polyoxometalate and Potassium Ion Framework for Enhanced Proton Conductivity. *Commun. Chem.* **2019**, *2*, 9.
(51) Iwano, T.; Miyazawa, S.; Uchida, S. Effect of Molecular weights of Confined Single-Chain Poly(allylamine) Toward Proton Conduction in Inorganic Frameworks Based on Preyssler-Type Polyoxometalate. *Inorg. Chim. Acta* **2020**, *499*, 119204.
(52) Iwano, T.; Shitamatsu, K.; Ogiwara, N.; Okuno, M.; Kikukawa, Y.; Ikemoto, S.; Shirai, S.; Muratsugu, S.; Waddell, P. G.; Errington, R. J.; Sadakane, M.; Uchida, S. Ultrahigh Proton Conduction via Extended Hydrogen-Bonding Network in a Preyssler-Type Polyoxometalate-Based Framework Functionalized with a Lanthanide Ion. *ACS Appl. Mater. Interfaces* **2021**, *13*, 19138.
(53) Almdal, K.; Dyre, J.; Hvidt, S.; Kramer, O. Towards a Phenomenological Definition of the Term 'Gel. *Polym. Gels Networks* **1993**, *1*, 5.
(54) Rubinstein, M.; Colby, R. H. *Polymer Physics*; OUP: Oxford, U.K., 2003.
(55) Nishinari, K. Some Thoughts on the Definition of a Gel. In *Gels: Structures, Properties, and Functions*; Kremer, F., Richtering, W., Eds.; Progress in Colloid and Polymer Science, Vol. *136*; Springer, 2009; pp 87−94, .
(56) Piepenbrock, M. O. M.; Lloyd, G. O.; Clarke, N.; Steed, J. W. Metal- and Anion-Binding Supramolecular Gels. *Chem. Rev.* **2010**, *110*, 1960.
(57) Yu, G. C.; Yan, X. Z.; Han, C. Y.; Huang, F. H. Characterization of Supramolecular Gels. *Chem. Soc. Rev.* **2013**, *42*, 6697.
(58) Mann, J. L.; Yu, A. C.; Agmon, G.; Appel, E. A. Supramolecular Polymeric Biomaterials. *Biomater. Sci-UK* **2018**, *6*, 10.
(59) Mezger, T. *The Rheology Handbook: For Users of Rotational and Oscillatory Rheometers*; Vincentz Network, 2020.
(60) Jing, B. X.; Xu, D. H.; Wang, X. R.; Zhu, Y. X. Multiresponsive, Critical Gel Behaviors of Polyzwitterion-Polyoxometalate Coacervate Complexes. *Macromolecules* **2018**, *51*, 9405.
(61) Carn, F.; Durupthy, O.; Fayolle, B.; Coradin, T.; Mosser, G.; Schmutz, M.; Maquet, J.; Livage, J.; Steunou, N. Assembling Vanadium(V) Oxide and Gelatin into Novel Bionanocomposites with Unexpected Rubber-like Properties. *Chem. Mater.* **2010**, *22*, 398.

https://doi.org/10.1021/acsmaterialslett.2c00393
ACS Materials Lett. 2022, 4, 1937−1943

(62) Zhang, S.; Shi, W.; Wang, X. Locking Volatile Organic Molecules by Subnanometer Inorganic Nanowire-Based Organogels. *Science* **2022**, *377*, 100.
(63) Terada, T.; Maeda, Y.; Kitano, H. Raman-Spectroscopic Study on Water in Polymer Gels. *J. Phys. Chem.* **1993**, *97*, 3619.
(64) Maeda, Y.; Tsukida, N.; Kitano, H.; Terada, T.; Yamanaka, J. Raman-Spectroscopic Study of Water in Aqueous Polymer-Solutions. *J. Phys. Chem.* **1993**, *97*, 13903.
(65) Ratajska-Gadomska, B.; Gadomski, W. Water Structure in Nanopores of Agarose Gel by Raman Spectroscopy. *J. Chem. Phys.* **2004**, *121*, 12583.
(66) Sekine, Y.; Ikeda-Fukazawa, T. Structural Changes of Water in a Hydrogel During Dehydration. *J. Chem. Phys.* **2009**, *130*, 034501.
(67) Kudo, K.; Ishida, J.; Syuu, G.; Sekine, Y.; Ikeda-Fukazawa, T. Structural Changes of Water in Poly(vinyl alcohol) Hydrogel During Dehydration. *J. Chem. Phys.* **2014**, *140*, 044909.
(68) Yoshihara, T.; Tadokoro, H.; Murahashi, S. Normal Vibrations of the Polymer Molecules of Helical Conformation. IV. Polyethylene Oxide and Polyethylene-d_4 Oxide. *J. Chem. Phys.* **1964**, *41*, 2902.
(69) Walrafen, G. E. Raman Spectral Studies of the Effects of Temperature on Water Structure. *J. Chem. Phys.* **1967**, *47*, 114.
(70) Colles, M. J.; Walrafen, G. E.; Wecht, K. W. Stimulated Raman spectra from H_2O, D_2O, HDO, and solutions of $NaClO_4$ in H_2O and D_2O. *Chem. Phys. Lett.* **1970**, *4*, 621.
(71) Walrafen, G. E., Raman and Infrared Spectral Investigations of Water Structure. In *The Physics and Physical Chemistry of Water*; Franks, F., Ed. Springer: New York, Boston, 1972; 151 pp.
(72) Green, J. L.; Lacey, A. R.; Sceats, M. G. Spectroscopic Evidence for Spatial Correlations of Hydrogen-Bonds in Liquid Water. *J. Phys. Chem.* **1986**, *90*, 3958.

https://doi.org/10.1021/acsmaterialslett.2c00393
ACS Materials Lett. 2022, 4, 1937−1943